Silicate and Salt Melts in the Genesis of the Industrial'noe Tin Deposit: Evidence from Inclusions in Minerals

V. B. Naumov[a] and V. S. Kamenetsky[b]

[a] *Vernadsky Institute of Geochemistry and Analytical Chemistry, Russian Academy of Sciences,
ul. Kosygina 19, Moscow, 119991 Russia*

e-mail: naumov@geokhi.ru

[b] *School of Earth Sciences and Centre for Ore Deposit Research, University of Tasmania, Hobart, Australia*

e-mail: Dima.Kamenetsky@utas.edu.au

Received April 14, 2005

Abstract—The data obtained on melt and fluid inclusions in minerals of granites, metasomatic rocks, and veins with tin ore mineralization at the Industrial'noe deposit in the southern part of the Omsukchan trough, northeastern Russia, indicate that the melt from which the quartz of the granites crystallized contained globules of salt melts. Silicate melt inclusions were used to determine the principal parameters of the magmatic melts that formed the granites, which had temperatures at 760–1020°C, were under pressures of 0.3–3.6 kbar, and had densities of 2.11–2.60 g/cm^3 and water concentrations of 1.7–7.0 wt %. The results obtained on the fluid inclusions testify that the parameters of the mineral-forming fluids broadly varied and corresponded to temperatures at 920–275°C, pressures 0.1–3.1 kbar, densities of 0.70–1.90 g/cm^3, and salinities of 4.0–75.0 wt % equiv. NaCl. Electron microprobe analyses of the glasses of twelve homogenized inclusions show concentrations of major components typical of an acid magmatic melt (wt %, average): 73.2% SiO_2, 15.3% Al_2O_3, 1.3% FeO, 0.6% CaO, 3.1% Na_2O, and 4.5% K_2O at elevated concentrations of Cl (up to 0.51 wt %, average 0.31 wt %). The concentrations and distribution of some elements (Cl, K, Ca, Mn, Fe, Cu, Zn, Pb, As, Br, Rb, Sr, and Sn) in polyphase salt globules in quartz from both the granites and a mineralized miarolitic cavity in granite were assayed by micro-PIXE (proton-induced X-ray emission). Analyses of eight salt globules in quartz from the granites point to high concentrations (average, wt %) of Cl (27.5), Fe (9.7), Cu (7.2), Mn (1.1), Zn (0.66), Pb (0.37) and (average, ppm) As (2020), Rb (1850), Sr (1090), and Br (990). The salt globules in the miarolitic quartz are rich in (average of 29 globules, wt %) Cl (25.0), Fe (5.4), Mn (1.0), Zn (0.50), Pb (0.24) and (ppm) Rb (810), Sn (540), and Br (470). The synthesis of all data obtained on melt and fluid inclusions in minerals from the Industrial'noe deposit suggest that the genesis of the tin ore mineralization was related to the crystallization of acid magmatic melts.

DOI: 10.1134/S0016702906120032

INTRODUCTION

Data obtained on inclusions in minerals are known to provide the most reliable quantitative information on the crystallization conditions and composition of the mineral-forming medium [1–12 and many others]. The world literature published over the past 15 years includes more than 5500 publications presenting data on inclusions in minerals. Recent years witnessed the most active examination of melt inclusions, which are unique in being able to preserve primary information of the physicochemical parameters, composition, and isotopic signatures of the corresponding natural magmatic systems. The reason for this extensive investigation of melt inclusions (Table 1) was the availability (in addition to thermometric methods) of modern analytical techniques of high spatial resolution, such as electron, ion, and proton microprobes.

We examined (using various analytical techniques) melt and fluid inclusions in minerals from granites, metasomatic rocks, and veins with tin ore mineraliza-tion from the Industrial'noe deposit in the southern part of the Omsukchan trough in northeastern Russia. The results of this research indicate that the magmatic silicate melt contained emulsion of salt melt globules, which did not mix with the silicate melt. We also managed to trace the evolution of the physicochemical

Table 1. Number of publications and analyses of melt inclusions examined on electron and ion microprobes

Period of time	Number	
	publications	analyses
1970–1974	6	99
1975–1984	43	408
1985–1994	160	1875
1995–2004	362	8350

parameters of the fluids from the earliest magmatic to late hydrothermal stages at this deposit.

GEOLOGICAL OVERVIEW

The Industrial'noe tin deposit in the southern part of the Omsukchan trough, northeastern Russia, is hosted by the leucocratic granites of the Levo-Omsukchan Massif, which is spatially restricted to a stratigraphic discontinuity between the complicatedly deformed terrigenous deposits of the Verkhoyansk Complex (T_3–J_2) and the gently dipping volcanic–sedimentary complex of the Omsukchan trough. The massif was produced by a succession of magmatic injections. Phase I gave rise to coarse- and medium-grained porphyritic biotite granites, which dominate in the massif. These rocks are cut by stocks and gently dipping bodies of phase-II fine-grained granites. Both of these phases are intersected by veins of aplites and aplitic granites. The phase-I granites were dated by the K–Ar method at 79 ± 4 Ma, and the basaltic dikes that cut across the veins with tin ore mineralization have an age of 77 ± 6 Ma [13].

The orebodies of tin mineralization are zones of metasomatically altered granites with thin filling veinlets in central parts. The rocks have a simple mineralogy and are characterized by a small number of mineralization stages. The oldest rocks of the deposit compose barren tourmalinization zones, which usually contain magnetite, quartz, and fluorite. The second stage was responsible for the formation of quartz, fluorite, sericite, chlorite, hematite, cassiterite, and, occasionally, pyrite. The minerals of the third (postmineral) stage include the fluorite of the filling veins 3–5 cm thick, late quartz, and the secondary minerals of the altered granites [13]. Interesting material was obtained from a mineralized cavity in the granite, which was exposed close to a vein with tin mineralization and reached 0.5 m across. The cavity contained large (up to 3–6 cm) crystals of quartz and tourmaline, and its walls were intersected by tourmaline veinlets.

The ore-forming process at the deposit was characterized by the active endogenic introduction of iron, as follows from chemical analyses of the chlorite metamomatites, which contain up to 29 wt % FeO (compared with 0.5–1.0 wt % FeO in the host granites). A noteworthy fact is the virtual absence of iron sulfides in the metasomatic rocks. More detailed information on the geology and mineralogy of the deposit are presented in [14, 15].

INCLUSIONS IN MINERALS

Methods used in studying inclusions in minerals. After the microscopical examination of polished platelets of the granites, quartz grains with melt inclusions were hand-picked from them. These grains were heated in a micromuffle with a Pt heater [16] to temperatures of 750–1050°C and were then rapidly quenched in air. The samples were held for 5–50 h. The glasses of melt inclusions thus obtained were exposed by polishing the mineral grains and analyzed on a Cameca SX50 microprobe equipped with four spectrometers at the University of Tasmania. The analytical conditions were as follows: 15 kV accelerating voltage, 15 nA beam current, and 5 μm beam diameter. The microprobe was calibrated on the compositions of natural glasses and mineral standards. To preclude Na losses during the analysis, the samples were first analyzed for this element for 10 s, and Si was analyzed simultaneously by another spectrometer.

The temperatures of fluid inclusions were measured on a stage designed by Kalyuzhnyi [17] accurate to ± 2°C (to 400°C) and ± 5°C (at 600–800°C).

The distribution of elements in inclusions and the concentrations of some elements were determined by micro-PIXE (proton-induced X-ray emission) at the CSIRO laboratory in North Ryde, Australia, by the method proposed in [18, 19]. This method makes use of high-energy (3 MeV) protons focused as a beam ~2 μm in diameter at a low beam current (0.3–0.7 nA). The concentrations were calculated with regard to the following parameters: size, geometry, and the overall density of the inclusions and the depth of the inclusions from the sample surface. The concentrations were measured accurate to 15–30%, with the errors increasing for light elements [20, 21] and depending on the inner structure of the inclusions (for example, the presence of daughter minerals) and their depth from the surface. It should be mentioned that the use of concentration ratios of elements with similar masses makes it possible to diminish the errors in the calculations and is recommended for geological interpretations. The compositional maps show the distributions of the concentrations of elements normalized to the maximum concentrations of these elements measured in a given individual inclusion. Because of this, the concentrations of various elements cannot be compared using the color compositional maps.

Melt inclusions. Primary melt inclusions were found in quartz from granites in all of our samples. The inclusions are normally less than 10 μm across but occasionally reach 20–40 μm. They consist (Fig. 1a) of a silicate material (anisotropic phases, one of which was determined to be muscovite) and fluid (aqueous solution and a gas bubble). The fluid phase of some melt inclusions contains cubic crystals, possibly halite (Fig. 1b). The fluid phase of some of the melt inclusions homogenizes to gas (at 310°C) or liquid (at 318–415°C), which suggests that the density of the fluid significantly varies, from 0.06 to 0.73 g/cm^3 (Table 2). The silicate phases start to melt at 680–700°C, but their heating to 650–660°C for even 5–6 h does not result in melting. Many melt inclusions contain small amounts of crystalline phases and gas bubbles even at 850–900°C (Fig. 1c). Complete homogenization was achieved for 250 inclusions at 760–1020°C, but most of the inclusions completely homogenized at
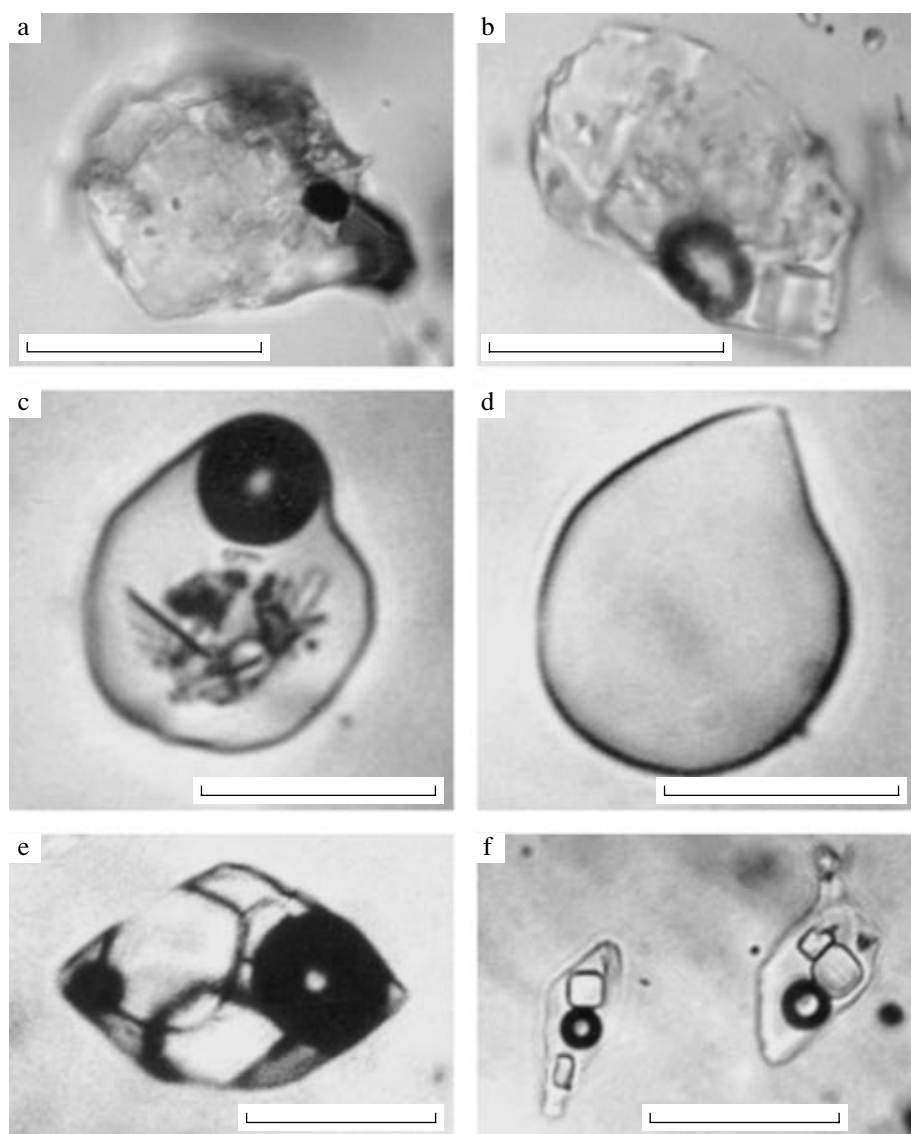
Fig. 1. Inclusions in quartz from granite: (a–d) melt inclusions; (a) Sample M-11, 20°C, the inclusion consists of silicate crystals, an ore mineral, and a fluid phase (gas bubble + aqueous solution); (b) sample M-11, 20°C, the fluid phase contains a cubic crystal, possibly halite; (c) sample M-11, 850°C; (d) same inclusion, 970°C; (e, f) fluid inclusions; (e) sample M-10, the solid phases include halite, sylvinite, and magnetite; (f) sample M-11, complete homogenization temperature is equal to 350°C. Scale bar is 20 µm.

850–950°C. Upon their quenching, these inclusions contained only homogenized silicate glass (Fig. 1d).

We also determined other parameters of the magmatic melts (Table 2) using the method in [22]. These parameters indicate that the crystallization of the massif occurred not only at a temperature decrease but also at variations of other parameters: the water concentration systematically varied from 1.7 to 7.0 wt %, the fluid pressure changed from 0.3 to 3.6 kbar, and the melt density changed from 2.11 to 2.60 g/cm³. We identified the following clearly pronounced tendency: the lower the water concentration and fluid pressure in the melt, the higher the homogenization temperature of the inclusions.

Table 3 lists chemical analyses of twelve homogenized melt inclusions from two granite samples (M-11 and M-20) from the lower and intermediate units, respectively. The SiO_2 concentration in the melt changed from 65.3 to 78.5 wt % at an average of 73.2 wt %. The contents of other major components are also typical of acid magmatic melts and are as follows (average, wt %): 15.3% Al_2O_3, 1.3% FeO, 0.02% MgO, 0.60% CaO, 3.1% Na_2O, and 4.5% K_2O. The P_2O_5 and S concentrations are very low, no higher than 0.01 wt %, but the rocks are characterized by elevated Cl concentrations (up to 0.51 wt % at an average of 0.31 wt %).

Fluid inclusions. The data obtained on fluid inclusions are summarized in Table 4, which reports the ranges of the principal parameters of these mineral-

Table 2. Principal parameters of magmatic melt: evidence from inclusions in quartz, Levo-Omsukchan Massif

Sample	Characteristics of the sample	Characteristics of fluid in recrystallized melt inclusions			Parameters of melt			
		homogenization temperature, °C	density, g/cm³	volume, vol %	water concentration, wt %	fluid pressure, kbar	density, g/cm³	temperature, °C
M-11	Quartz from coarse- medium-grained granite (lower unit)	310	0.06	22.5	1.7	0.3	2.11	1020–760
		415	0.46	12.7	3.3	1.6	2.41	
M-20	Quartz from medium-grained granite (middle unit)	345	0.67	20.7	6.8	3.1	2.28	
		318	0.73	20.0	7.0	3.6	2.31	
M-2	Quartz from coarse- medium-grained granite (upper unit)	388	0.55	4.6	1.9	2.0	2.60	

Table 3. Chemical composition (wt %) of glasses from melt inclusions in quartz from granites of the Levo-Omsukchan Massif

Component	1	2	3	4	5	6	7	8	9	10	11	12
SiO_2	69.90	70.92	73.12	73.97	74.98	75.55	76.06	76.74	65.33	67.81	75.32	78.45
TiO_2	0.17	0.06	0.13	0.11	0.10	0.04	0.09	0.11	0.01	0.00	0.24	0.20
Al_2O_3	18.12	18.08	15.84	15.85	13.84	13.32	13.75	13.13	18.93	19.11	13.54	10.16
FeO	1.90	0.45	1.46	1.35	1.36	1.17	1.28	1.28	0.54	0.12	1.78	2.49
MnO	0.04	0.03	0.07	0.04	0.05	0.04	0.03	0.05	0.05	0.00	0.01	0.12
MgO	0.04	0.01	0.01	0.01	0.04	0.01	0.01	0.03	0.02	0.00	0.05	0.02
CaO	1.28	0.49	0.86	0.80	0.64	0.49	0.56	0.56	0.30	0.20	0.54	0.37
Na_2O	3.08	4.08	2.70	1.89	2.86	2.68	2.75	2.91	4.84	6.82	1.65	1.06
K_2O	4.44	3.53	4.47	4.40	3.18	3.16	4.23	3.28	7.60	6.25	4.80	4.35
P_2O_5	0.00	0.00	0.00	0.00	0.01	0.00	0.00	0.00	0.00	0.00	0.01	0.00
Cl	0.42	0.05	0.36	0.36	0.43	0.36	0.29	0.33	0.05	0.03	0.51	0.51
S	0.00	0.01	0.00	0.00	0.01	0.00	0.01	0.01	0.01	0.03	0.01	0.00
Total	99.37	97.69	99.03	98.80	97.40	96.76	99.06	98.35	97.76	100.36	98.46	97.74

Note: Platelets with melt inclusions were held in a muffle at 950°C for 20 h and were then quenched in air. Analyses 1–8 are from sample M-11, analyses 9–12 are from sample M-20.

forming fluids: temperature, pressure, density, and salinity. Polyphase fluid inclusions were found in quartz from the granites (Figs. 1e and 1f), quartz and fluorite from the mineralized cavity in granite (Fig. 2), quartz from the quartz–tourmaline metasomatites, and in quartz and fluorite from veins with tin mineralization and crystalline aggregates. Solid phases account for 5–80 vol % of the inclusions, and their amount varies from one to ten. The only minerals identified in them are halite, sylvinite, and magnetite. Some of the inclusions were dominated by gas and were likely captured during the heterogenizaton of the solutions. These inclusions are most typical of quartz from the mineralized veins (samples 2697 and 26104).

Most of the daughter crystals of the polyphase inclusions dissolve at temperatures below 300–350°C: the first crystal usually dissolves at 55–60°C, the second one at 130–150°C, and the third and fourth crystals dissolved in the temperature range of 250–350°C. The large isotropic crystal (halite) dissolved in individual inclusions at temperatures from 300 to 625°C. It should be mentioned that most inclusions, particularly large ones, decrepitate before their complete homogenization, with this process being the most active at 570–580°C.

The overall range of the homogenization temperatures of the fluid inclusions is unusually broad, from 920 to 275°C, and Table 4 does not list data on obviously secondary two-phase inclusions in fluorite from sample 26122, which homogenized at 175–160°C. The maximum homogenization temperatures of the fluid inclusions in each group of the rocks are obviously prone to decrease: 920°C for the granites, 840°C for the mineralized cavity in granite, 550°C for the quartz–tourmaline metasomatic rocks, and 465°C for the mineralized veins. Since the lower limit of the magmatic melt temperature was assayed from melt inclusions at 760°C (Table 2), it is reasonable to suggest that the silicate melt coexisted with a hydrothermal fluid within a

Table 4. Data on fluid inclusions in minerals from the Industrial'noe tin deposit

Sample	Characteristics of the sample	Mineral	Characteristics of mineral-forming fluid			
			tempera-ture, °C	pressure, kbar	density, g/cm^3	salinity*
M-11	Granite (lower unit)	Quartz**	810–340	3.10–0.40	1.28–0.90	52.5–41.0
M-20	Granite (middle unit)	Quartz**	920–485	2.40–0.87	1.63–1.16	71.0–45.0
M-10	Granite (middle unit)	Quartz**	850–415	1.80–0.50	1.55–0.24	72.5–13.3
M-2	Granite (upper unit)	Quartz**	680–365	2.30–0.77	1.70–0.54	74.0–43.5
M-17	Granite (upper unit)	Quartz**	570–340	1.60–0.25	1.58–0.90	73.0–40.5
2541	Cluster of quartz, tourmaline, and fluorite crystals from a cavity in granite (middle unit)	Fluorite**	710–475	2.5	1.80–1.65	70.0–40.0
		Quartz**	840–315	2.50–1.05	1.90–0.94	75.0–35.0
25140	Quartz–tourmaline aggregate from granite	Quartz**	550–305	1.20–0.36	1.08–0.88	54.0–35.5
26116	Quartz–tourmaline aggregate from a vein with tin mineralization	Quartz	530–355	2.00–0.90	1.68–1.05	70.0–42.0
26115	same	Quartz	490–370	1.60–0.75	1.47–0.92	66.0–39.0
2697	Quartz–cassiterite vein 5	Quartz	465–385	1.1–0.27	1.20–0.92	60.0–35.6
26104	Quartz–cassiterite vein 13	Quartz	360–275	0.35–0.12	1.08–1.00	36.0–35.6
2415	Quartz–tourmaline–fluorite aggregate	Fluorite**	445–395	0.55	1.63–1.05	64.0–43.0
26122	Cluster of fluorite crystals from vein 7	Fluorite	420–325	–	1.73–0.70	65.0–4.0
25105	Cluster of fluorite crystals from a vein in the lower unit	Fluorite**	375–300	–	1.14–0.94	44.0–29.0

 * Wt % equiv. NaCl.
** Fluid inclusions contain daughter magnetite.

temperature range of 920–760°C. Hence, this was a magmatic-stage fluid. These data also imply that minerals started to crystallize in the cavity in granite during the magmatic stage but only from fluid.

When the temperatures of phase transitions in polyphase fluid inclusions are examined, the gas phase very often disappeared (partial homogenization) before the complete dissolution of the solid phase (complete homogenization). This situation makes it possible to pinpoint the pressure during complete homogenization by the method proposed in [23]. It should be mentioned that the inclusions selected for these measurements had identical phase composition but differed in size. Complete homogenization could commonly be accomplished only for relatively small inclusions, because the high internal pressures resulted in the decrepitation of many inclusions long before their homogenization. As can be seen from the data of Table 4, the overall pressure range is quite significant: from 3.1 to 0.1 kbar. Similarly to the homogenization temperatures, the fluid pressures also tend to gradually decrease for rock groups: 3.1 kbar for the granites, 2.5 kbar for the mineralized cavity in the granites, 2.0 kbar for the quartz–tourmaline metasomatic rocks, and 1.1 kbar for the mineralized veins.

In the polyphase fluid inclusions, the solid phases are volumetrically dominated by Na and K chlorides. Using the dissolution temperatures of sylvinite and halite and data on solubility in the H_2O–NaCl and H_2O–NaCl–KCl systems [24, 25], one can assay the salinity of the mineralizing fluid. The results presented in Table 4 indicate that the salinity of most of the solutions is much greater than 30 wt % equiv. NaCl and reaches 75 wt % equiv. NaCl. Only one fluorite sample (sample 26122) contained a fluid inclusion with a homogenization temperature of 325° which, according to our cryometric data, contained solution with a salinity of 4.0 wt % equiv. NaCl.

As was mentioned above, the mineralizing process at the deposit was characterized by the active endogenic introduction of iron. This was corroborated by the data obtained on fluid inclusions in the quartz and fluorite. Many samples (Table 4) had inclusions with strongly magnetic daughter minerals, perhaps, magnetite, which accounted for as much as 0.5–3.2 vol % of the inclusions. The Fe concentration was estimated in the inclusions at 15–75 g/kg of solution by the method [26] (eight measurements). It is pertinent to note that an equally high Fe concentration (18 g/kg of solution) was documented in chloride solutions at the Araca tin deposit in Bolivia and
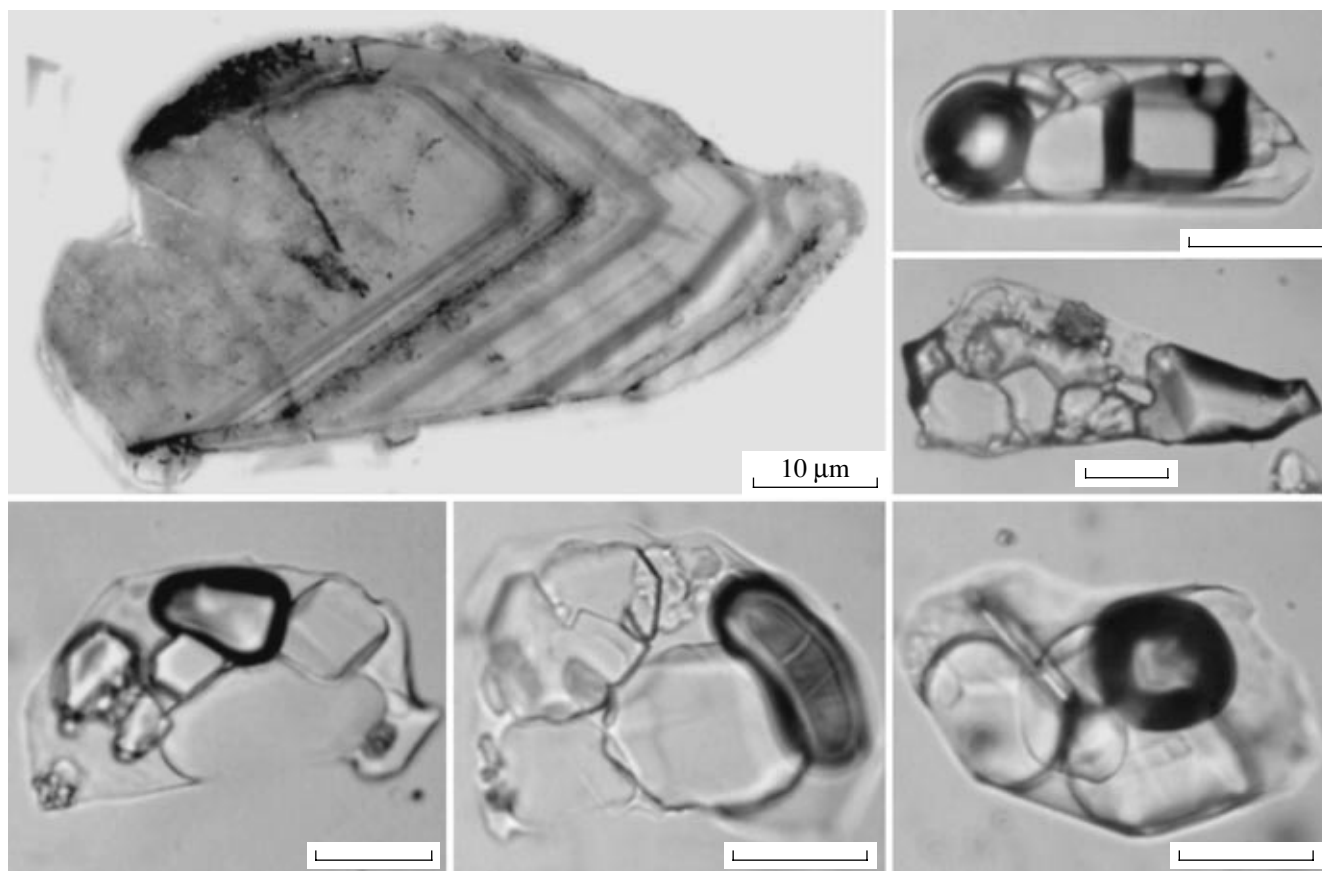
Fig. 2. Quartz crystal from a cavity in granite and a polyphase inclusion in the core of this crystal. Scale bar is 10 μm.

in chloride solutions at the Tyrny-Auz deposit in the Northern Caucasus (73 ± 21 g/kg of solution) [26].

The high salinity of mineral-forming fluids at the Industrial'noe deposit unambiguously testifies to their high density. Studying inclusions in minerals makes it possible to assay this parameter on the basis of experimentally determined densities of the gas, liquid, and solid phases identified in the inclusions. Estimating the densities and volumes of each of the phases, the researcher can then calculate the density of the fluid captured during the crystallization of the mineral. The results of these estimates are summarized in Table 4. The overall range of these estimates is quite broad, from a relatively low density value of 0.24 g/cm^3 to extremely high ones, up to 1.90 g/cm^3. Most of the individual estimates exceed 1.0 g/cm^3.

Salt melts. After the polished quartz platelets were held for up to 20 h at a high temperature (950°C) and were then rapidly quenched in air, they were examined under a microscope (see above). In addition to melt inclusions yielding homogeneous glass (Fig. 1d and Table 3), some quartz grains were determined to bear melt inclusions with variable amounts of salt globules (Fig. 3). This fact suggests that the silicate melt contained droplets (emulsion) of salt melts when quartz crystallized from this silicate melt. Droplets of the salt melts were more often entrapped by growing quartz grains together with the silicate melt (at variable proportions of the melts), although salt globules could be occasionally conserved in the quartz without silicate melt. Analogous (but larger) salt melt inclusions were found in the core of a quartz crystal from the cavity (Fig. 2).

The distribution of elements in the inclusions and the concentrations of some elements were analyzed by micro-PIXE. Figure 4a presents data on the distribution of elements in a silicate melt inclusion with a salt globule in its central part, and Fig. 4b shows the distribution of these elements in a fluid inclusion with numerous daughter phases. Analogous distribution patterns of elements in other inclusions were published in our earlier papers [27, 28]. We analyzed eight salt globules in quartz from the granite and 29 salt globules in quartz from the cavity in granite. The results of the analyses are presented in Table 5. Note the significant differences in the concentrations of some elements in the salt globules in quartz from the granite and in this mineral from the cavity in these rocks. These concentrations are as follows: 7.21 wt % (average of eight analyses) and 0.02 wt % (average of 29 analyses) for Cu, 2020 and 226 ppm for As, 1360 and 290 ppm for Ti, and 1090 and 253 ppm for Sr. At the same time, the concentrations of
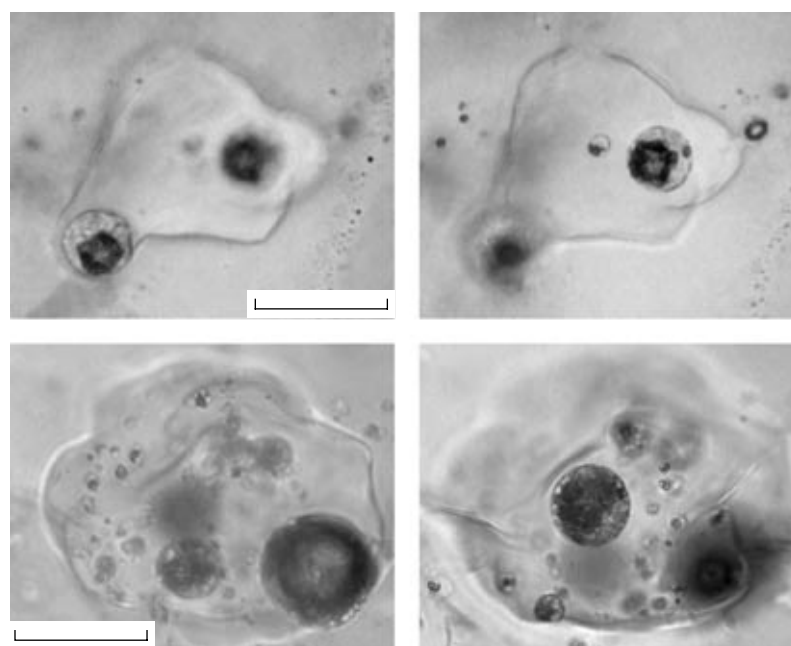
Fig. 3. Melt inclusions in quartz from granite after heating to 950°C for 20 h and rapid quenching. The inclusions consist of silicate glass and variable numbers of spherical salt globules. Scale bar is 20 μm.
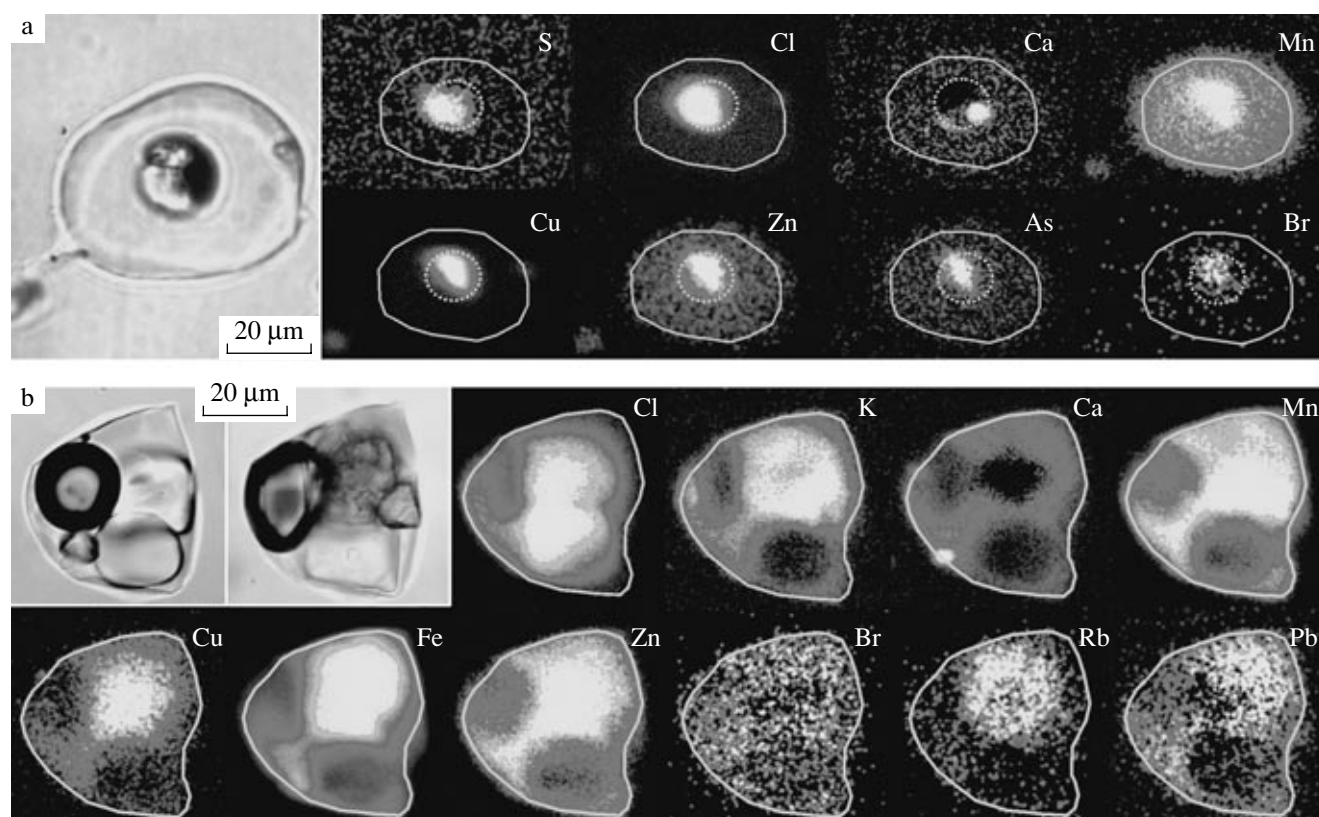

Fig. 4. Compositional maps of various elements (PIXE imagery). (a) Melt inclusion in quartz from granite. The inclusion consists of silicate glass and a salt globule. (b) Fluid inclusion in quartz from the cavity.

Table 5. Chemical composition of salt globules in quartz from granite and a cavity in granite at the Industrial'noe tin deposit

Sample	wt %								ppm					
	Cl	K	Ca	Mn	Fe	Cu	Zn	Pb	As	Ti	Br	Rb	Sr	Sn
1	54	–	0.53	0.71	–	3.71	0.49	0.47	1220	–	1080	2050	970	–
2	15	–	0.78	0.73	–	6.02	0.48	0.34	467	–	1450	–	–	–
3	43	–	2.68	1.17	–	15.4	0.43	0.17	4300	–	900	3480	–	–
4	53	–	0.90	1.05	–	22.2	0.47	0.23	6550	–	800	3620	3290	–
5	7	1.6	0.90	0.76	4.04	2.47	0.48	0.21	1160	–	590	510	400	–
6	12	2.9	1.88	1.35	7.38	3.61	0.82	0.37	2030	–	1040	1770	590	–
7	24	5.0	1.51	2.06	19.3	2.90	1.34	0.71	281	–	1300	3260	869	–
8	12	2.9	0.88	1.24	7.89	1.31	0.80	0.48	161	–	786	1180	427	–
9	40.5	5.8	1.60	0.96	5.10	0.03	0.42	0.21	–	110	382	637	98	264
10	55.3	19	3.10	1.90	8.70	0.03	1.00	0.50	–	137	703	1000	309	626
11	24.9	5.4	0.72	1.14	4.86	0.02	1.81	6.98	502	151	2000	641	–	421
12	39.5	6.8	3.56	1.75	9.81	0.05	0.96	0.38	16	400	751	1190	446	586
13	31.9	4.4	0.46	0.70	4.62	0.03	0.34	0.44	–	278	250	808	–	231
14	34.5	3.0	0.41	0.86	6.00	0.02	0.42	0.18	533	109	383	1100	–	860
15	44.5	10	3.86	1.63	7.20	0.04	0.80	0.15	190	28	582	317	164	388
16	12.7	3.6	0.69	0.58	2.74	0.01	0.32	0.13	45	40	269	339	120	392
17	39.2	13	1.80	3.05	19.6	0.09	1.58	0.74	1100	354	1500	3400	–	1700
18	47.7	6.1	1.75	1.42	7.61	0.03	0.63	0.33	–	147	255	357	212	604
19	35.3	6.7	0.78	1.16	8.06	0.07	0.70	0.25	124	305	511	1400	–	1200
20	27.5	3.1	1.26	1.13	9.66	7.21	0.66	0.37	2020	1360	993	1850	1090	–
21	25.0	5.4	1.30	1.00	5.40	0.02	0.50	0.24	226	209	472	807	253	537

Note: (1–8) Salt globules in quartz from granite (1–4—salt globules in melt inclusions in quartz from granite, 5–8—salt globules in quartz from granite); (9–19) salt globules in melt inclusions in quartz from the cavity; (20) average composition of eight salt globules in quartz from granite; (21) average composition of 29 salt globules in quartz from a cavity in granite.

Cl, K, Ca, Mn, Zn, and Pb are roughly equal in both quartz types. The high Fe concentration in analyses of the salt globules (from 5.4 to 9.7 wt % on average, Table 5) are in good agreement with our earlier estimates of the equally high Fe concentrations for fluid inclusions in the quartz and fluorite (15–75 g/kg of solution). It is also worth mentioning the high Sn concentrations in the salt globules: from 230 to 1700 ppm (average 537 ppm).

The coexistence of silicate and salt melts was documented by many researchers for various natural magmatic rocks [29–43 and others]. The paper by Roedder and Coombs [29] seems to be the first (it was published in 1967) to present detailed data on inclusions in quartz and feldspar from granite blocks at Ascension Island. These materials provided convincing evidence for the possibility of the coexistence of two immiscible phases: silicate and chloride salt melts (with a density of ~1.4 g/cm³). Salt melts of predominantly chloride composition were found in many magmatic rocks together with silicate melts [30, 32, 35, 37, 39, 43, and others]. The composi-

tion of the salt melts can broadly vary depending on the geological setting. For example, the melts can be dominated by fluorides [33]; phosphates and sulfates [34]; carbonates, sulfates, fluorides, and chloride [36]; phosphates and silicates [40]; fluorides with sulfate and chlorides with sulfates [41]; and sulfates with carbonates [42]. Note that while the predominant components of the chloride melts are Na and K, salt melts of other compositions are dominated by Ca.

In conclusion of the discussion of our results obtained on melt and fluid inclusions in minerals from the Industrial'noe deposit, it should be noted that these data are completely consistent with our earlier conclusion [15, 44–46] that the processes that produce rare-metal ore mineralization are genetically related to the crystallization of acid melts. The principal compositional features and concentrations of the solutions participating in the ore-forming process are undoubtedly formed during the magmatic and early postmagmatic stages.

CONCLUSIONS

1. The data obtained on silicate melt inclusions in quartz from the granites allowed us to determine the principal parameters of the magmatic melts: temperatures of 760–1020°C, fluid pressures of 0.3–3.6 kbar, densities of 2.11–2.60 g/cm^3, and water contents of 1.7–7.0 wt %. Electron-microprobe analyses of glasses from twelve homogenized inclusions show major-element concentrations typical of acid magmatic melts (wt %, on average): 73.2% SiO$_2$, 15.3% Al$_2$O$_3$, 1.3% FeO, 0.6% CaO, 3.1% Na$_2$O, and 4.5% K$_2$O at elevated concentrations of Cl (up to 0.51 wt %, 0.31 wt % on average).

2. Our data on fluid inclusions in quartz and fluorite suggest broad variations in the parameters of the mineral-forming fluids at the deposit: the temperature varied from 920 to 275°C, pressure from 3.1 to 0.1 kbar, density from 1.90 to 0.70 g/cm^3, and salinity from 75.0 to 4.0 wt % equiv. NaCl.

3. It was established that, when quartz crystallized from the silicate granitic melt, the latter contained emulsion of salt melt droplets. These droplets were more often captured by growing quartz crystals together with the silicate melt, and the proportions of the two melts varied, with salt droplets (globules) occasionally entrapped in quartz alone, without silicate melt. The concentrations and distributions of 13 elements in polyphase salt globules found in quartz from both the granites and a cavity in them were determined by PIXE. Analyses of eight salt globules in quartz from the granites show high concentrations (wt %, average) of Cl (27.5), Fe (9.7), Cu (7.2), Mn (1.1), Zn (0.66), Pb (0.37) and (ppm, average) As (2020), Rb (1850), Sr (1090), and Br (990). The salt globules in quartz from the cavity are also rich in (wt %, average of 29 globules) Cl (25.0), Fe (5.4), Mn (1.0), Zn (0.50), Pb (0.24), and (ppm) Rb (810), Sn (540), and Br (470). The data obtained on melt and fluid inclusions in minerals from the Industrial'noe deposit led us to conclude that the genesis of the tin ore mineralization was related to the crystallization of the acid magmatic melts.

REFERENCES

1. N. P. Ermakov, *Studies of Mineral-Forming Solutions* (Khar'k. Univ., Khar'kov, 1950) [in Russian].

2. R. Clocchiatti, "Composition chimique des inclusions vitreuses des phenocristaux de quartz de quelques laves acides par l'analyse a la sonde electronique," C. R. Acad. Sci. Paris **272**, 2045–2047 (1971).

3. G. G. Lemmlein, *Morphology and Genesis of Crystals* (Nauka, Moscow, 1973) [in Russian].

4. T. Yu. Bazarova, I. T. Bakumenko, V. P. Kostyuk, et al., *Magmatic Crystallization Based on Melt Inclusion Data* (Nauka, Novosibirsk, 1975) [in Russian].

5. V. B. Naumov and G. B. Naumov, "Mineral-Forming Fluids and Physicochemical Characteristics of Their Evolution," Geokhimiya, No. 10, 1450–1460 (1980).

6. E. Roedder, "Fluid Inclusions," Rev. Mineral. **12**, (1984).

7. V. B. Naumov and V. I. Kovalenko, "Characteristics of Major Volatiles of Natural Magmas and Metamorphic Fluids Based on Mineral Inclusion Data," Geokhimiya, No. 5, 590–600 (1986).

8. A. T. Anderson, Jr., "Hourglass Inclusions: Theory and Application to the Bishop Rhyolitic Tuff," Am. Mineral. **76**, 530–547 (1991).

9. A. V. Sobolev, "Melt Inclusions in Minerals as a Source of Principal Petrological Information," Petrologiya **4**, 228–239 (1996) [Petrology **4**, 209–220 (1996)].

10. J. D. Webster, D. M. Burt, and R. A. Aguillon, "Volatile and Lithophile Trace-Element Geochemistry of Mexican Tin Rhyolite Magmas Deduced from Melt Inclusions," Geochim. Cosmochim. Acta **60**, 3267–3283 (1996).

11. V. B. Naumov, V. I. Kovalenko, V. A. Dorofeeva, and V. V. Yarmolyuk, "Average Concentrations of Major, Volatile, and Trace Elements in Magmas of Various Geodynamic Settings," Geokhimiya, No. 10, 1113–1124 (2004) [Geochem. Int. **42**, 977–987 (2004)].

12. M. B. Kamenetsky, A. V. Sobolev, V. S. Kamenetsky, et al., "Kimberlite Melts Rich in Alkali Chlorides and Carbonates: A Potent Metasomatic Agent in the Mantle," Geology **32**, 845–848 (2004).

13. A. L. Sokolov, "Metasomatic Zoning at the Industrial'noe–Khatarenskoe Ore Field (Omsukchan District)," Geol. Rudn. Mestorozhd., No. 2, 27–35 (1980).

14. A. L. Sokolov, "Localization Conditions of the Cassiterite–Silicate Mineralization: Evidence from the Industrial'noe Deposit," Izv. Akad. Nauk SSSR, Ser. Geol., No. 9, 121–132 (1980).

15. V. B. Naumov and A. L. Sokolov, "Genetic Relations of Granites and the Tin Veins of the Industrial'noe Deposit: Inclusion in Mineral Data," Geol. Rudn. Mestorozhd., No. 4, 74–80 (1981).

16. V. B. Naumov, "Thermometric Study of Melt Inclusions in Quartz Phenocrysts from Quartz Porphyries," Geokhimiya, No. 4, 494–498 (1969).

17. V. A. Kalyuzhnyi, "Improvement of Microscopic Thermal Stage for the Analysis of Liquid Inclusions," Tr. Vsesoyuz. Nauchn.-Issled. Inst. P'ezosyr. **2** (2), 43–47 (1958).

18. C. G. Ryan, B. M. McInnes, P. J. Williams, et al., "Imaging Fluid Inclusion Content Using the New CSIRO–GEMOC Nuclear Microprobe," Nucl. Instr. Methods Phys. Res. **181**, 570–577 (2001).

19. C. G. Ryan, E. van Achterbergh, W. L. Griffin, et al., "Nuclear Microprobe Analysis of Melt Inclusions in Minerals: Windows on Metasomatic Processes in the Earth's Mantle," Nucl. Instr. Methods Phys. Res. **181**, 578–585 (2001).

20. C. G. Ryan, C. A. Heinrich, E. van Achterbergh, et al., "Microanalysis of Ore-Forming Fluids Using the Scanning Proton Microprobe," Nucl. Instr. Methods Phys. Res. **104**, 182–190 (1995).

21. M. Kurosawa, S. Shimano, S. Ishii, and T. Kato, "Quantitative Trace Element Analysis of Single Fluid Inclusions by Proton-Induced X-Ray Emission (PIXE):

Application to Fluid Inclusions in Hydrothermal Quartz," Geochim. Cosmochim. Acta **67**, 4337–4352 (2003).

22. V. B. Naumov, "Determination of Concentrations and Pressure of Volatiles in Magmatic Melts on the Basis of Inclusions in Minerals," Geokhimiya, No. 7, 997–1007 (1979).

23. P. V. Klevtsov and G. G. Lemmlein, "Determination of the Minimum Pressure of Quartz Formation as Exemplified by Crystals from the Pamirs," Zap. Vses. Mineral. O–va **88**, 661–666 (1959).

24. E. Roedder, "Fluid Inclusion Studies on the Porphyry-Type Ore Deposits at Bingham, Utah, Butte, Montana, and Climax," Econ. Geol. **66**, 98–120 (1971).

25. S. Sourirajan and G. C. Kennedy, "The System H_2O–NaCl at Elevated Temperatures and Pressures," Am. J. Sci. **260**, 115–141 (1962).

26. V. B. Naumov and V. V. Shapenko, "Iron Concentrations in the Chloride Solutions Based on Mineral Inclusion Data," Geokhimiya, No. 2, 231–238 (1980).

27. V. S. Kamenetsky, E. van Achterbergh, C. G. Ryan, et al., "Extreme Chemical Heterogeneity of Granite-Derived Hydrothermal Fluids: An Example from Inclusions in a Single Crystal of Miarolitic Quartz," Geology **30**, 459–462 (2002).

28. V. S. Kamenetsky, V. B. Naumov, P. Davidson, et al., "Immiscibility between Silicate Magmas and Aqueous Fluids: A Melt Inclusion Pursuit into the Magmatic–Hydrothermal Transition in the Omsukchan Granite (NE Russia)," Chem. Geol. **210**, 73–90 (2004).

29. E. Roedder and D. S. Coombs, "Immiscibility in Granitic Melts, Indicated by Fluid Inclusions in Ejected Granitic Blocks from Ascension Island," J. Petrol. **8**, 417–451 (1967).

30. F. G. Reyf and E. D. Bazheyev, "Magmatic Chloride Solution and Tungsten Mineralization," Geochem. Int. **14**, 45–51 (1977).

31. O. N. Kosukhin, "Genesis of Graphic Textures," Geol. Geofiz., No. 4, 46–50 (1981).

32. V. B. Naumov, V. I. Kovalenko, and L. G. Filimonova, "Immiscibility of Silicate and Salt Melts as Indicated by Mineral Inclusion Data," in *Proceedings of 10th Seminar on Geochemistry of Magmatic Rocks, Moscow, Russia, 1984* (Moscow, 1984), pp. 130–131 [in Russian].

33. V. B. Naumov, V. I. Kovalenko, A. V. Sobolev, et al., "Immiscibility between Silicate and Salt Melts: Evidence from Mineral Inclusions in High-Temperature Fluorite," Dokl. Akad. Nauk SSSR **288**, 453–456 (1986).

34. V. B. Naumov, I. P. Solovova, V. I. Kovalenko, et al., "Natural Phosphate–Sulfate Melts," Dokl. Akad. Nauk SSSR **300**, 672–675 (1988).

35. V. B. Naumov, I. P. Solovova, V. A. Kovalenker, et al., "Crystallization Conditions and Compositions of Silicate and Salt Melts of the Volcanoplutonic Complex in the Angren Area, Soviet Central Asia," Dokl. Akad. Nauk. SSSR **312**, 199–202 (1990).

36. I. P. Solovova, A. V. Girnis, A. V. Guzhova, and V. B. Naumov, "Magmatic Salt Inclusions in East Pamir Alkali Basalt Minerals," Geochem. Int. **29** (8), 64–74 (1992).

37. M. L. Frezzotti, "Magmatic Immiscibility and Fluid Phase Evolution in the Mount Genis Granite (Southeastern Sardinia, Italy)," Geochim. Cosmochim. Acta **56**, 21–33 (1992).

38. E. Roedder, "Fluid Inclusion Evidence for Immiscibility in Magmatic Differentiation," Geochim. Cosmochim. Acta **56**, 5–20 (1992).

39. J. B. Lowenstern, "Chlorine, Fluid Immiscibility, and Degassing in Peralkaline Magmas from Pantelleria, Italy," Am. Mineral. **79**, 353–369 (1994).

40. I. A. Andreeva, V. B. Naumov, V. I. Kovalenko, and N. N. Kononkova, "Natural Phosphate–Silicate Melts," Dokl. Akad. Nauk **343**, 237–241 (1995).

41. I. A. Andreeva, V. B. Naumov, V. I. Kovalenko, and N. N. Kononkova, "Fluoride–Sulfate and Chloride–Sulfate Salt Melts of the Mushugai-Khuduk Carbonatite-Bearing Complex, Southern Mongolia," Petrology **6**, 284–292 (1998).

42. L. I. Panina and L. M. Usol'tseva, "Alkaline High-Ca Sulfate–Carbonate Melt Inclusions in Melilite–Monticellite–Olivine Rocks from the Malomurunskii Alkaline Massif, Aldan," Petrology **7**, 610–625 (1999).

43. P. Davidson and V. S. Kamenetsky, "Immiscibility and Continuous Felsic Melt–Fluid Evolution within the Rio Blanco Porphyry System, Chile: Evidence from Inclusions in Magmatic Quartz," Econ. Geol. **96**, 1921–1929 (2001).

44. V. B. Naumov and G. F. Ivanova, "Geochemical Criteria for the Genetic Relationship of Rare-Metal Mineralization with Acid Magmatism," Geokhimiya, No. 6, 791–804 (1984).

45. V. B. Naumov and G. F. Ivanova, "Genetic Relationship between Rare-Metal Mineralization and Acid Magmatism as Revealed by the Study of Microinclusions and Indicator Microcomponents," in *Proceedings of 6th IAGOD Symposium, Stuttgart, Germany, 1984* (Stuttgart, 1984), pp. 395–401.

46. V. B. Naumov, V. I. Kovalenko, and V. A. Dorofeeva, "Magmatic Volatile Components and Their Role in the Formation of Ore-Forming Fluids," Geol. Rudn. Mestorozhd. **39**, 520–529 (1997) [Geol. Ore Dep. **39**, 451–460 (1997)].